# Anti–IL-20 monoclonal antibody inhibits the differentiation of osteoclasts and protects against osteoporotic bone loss

Yu-Hsiang Hsu,[1,2] Wei-Yu Chen,[2] Chien-Hui Chan,[2] Chih-Hsing Wu,[3] Zih-Jie Sun,[3] and Ming-Shi Chang[1,2]

[1]Institute of Biopharmaceutical Sciences, [2]Department of Biochemistry and Molecular Biology, and [3]Department of Family Medicine, College of Medicine, National Cheng Kung University, Tainan City 701, Taiwan

**IL-20 is a proinflammatory cytokine of the IL-10 family that is involved in psoriasis, rheumatoid arthritis, atherosclerosis, and stroke. However, little is known about the role of IL-20 in bone destruction. We explored the function of IL-20 in osteoclastogenesis and the therapeutic potential of anti–IL-20 monoclonal antibody 7E for treating osteoporosis. Higher serum IL-20 levels were detected in patients with osteopenia and osteoporosis and in ovariectomized (OVX) mice. IL-20 mediates osteoclastogenesis by up-regulating the receptor activator of NF-κB (RANK) expression in osteoclast precursor cells and RANK ligand (RANKL) in osteoblasts. 7E treatment completely inhibited osteoclast differentiation induced by macrophage colony-stimulating factor (M-CSF) and RANKL in vitro and protected mice from OVX-induced bone loss in vivo. Furthermore, IL-20R1–deficient mice had significantly higher bone mineral density (BMD) than did wild-type controls. IL-20R1 deficiency also abolished IL-20–induced osteoclastogenesis and increased BMD in OVX mice. We have identified a pivotal role of IL-20 in osteoclast differentiation, and we conclude that anti–IL-20 monoclonal antibody is a potential therapeutic for protecting against osteoporotic bone loss.**

CORRESPONDENCE
Ming-Shi Chang:
mschang@mail.ncku.edu.tw

Abbreviations used: BMD, bone mineral density; CIA, collagen-induced arthritis; CTX, C-terminal telopeptide of collagen; HSC, hematopoietic stem cell; micro-CT, micro-computed tomography; OC CM, osteoclast conditioned medium; OVX, ovariectomized; RA, rheumatoid arthritis; RANK, receptor activator of NF-κB; RANKL, RANK ligand; TRAP, tartrate-resistant acid phosphatase.

Bone resorption is a major pathological factor in chronic inflammatory diseases such as rheumatoid arthritis (RA), periodontitis, and osteoporosis. Osteoporosis is a disorder of impaired bone strength that causes skeletal fragility and increases the risk of fractures (Theill et al., 2002; Boyle et al., 2003). An estrogen deficiency at menopause and an androgen deficiency in men both cause an unbalanced increase in bone turnover, in which bone resorption exceeds bone formation. Relatively rapid bone loss occurs and is accompanied by the destruction of bone micro-architecture (Simonet et al., 1997; McClung, 2007). In most instances, low bone mass is caused by an increase in the number of osteoclasts or by excessive osteoclast activity (Walsh et al., 2005). Osteoclasts are multinucleated giant cells that express tartrate-resistant acid phosphatase (TRAP) and calcitonin receptors. Osteoclast formation requires macrophage (M) CSF and receptor activator of NF-κB (RANK) ligand (RANKL; Ross and Teitelbaum, 2005; Takayanagi et al., 2005). M-CSF, which mediates the survival and proliferation of monocyte/macrophage precursors, is produced primarily by stromal fibroblasts, osteoblasts, and activated T cells. RANK is the sole signaling receptor for RANKL, which induces the development and activation of osteoclasts (Suda et al., 1999). The in vivo significance of the RANKL–RANK signaling pathway has been verified by observations that the deficiency of either gene in mice causes severe osteopetrosis (increased bone mass) and the disappearance of osteoclasts (Kong et al., 1999; Li et al., 2000). Several proinflammatory cytokines, such as TNF, IL-1β, IL-15, IL-17, and IL-23, induce the multinucleation of osteoclast precursors, or their commitment to the osteoclast phenotype, and may act synergistically with RANKL (Feldmann et al., 2001; O'Gradaigh et al., 2004; Sato et al., 2006; Ju et al., 2008; O'Brien, 2010).

The pleiotropic inflammatory cytokine IL-20, a member of the IL-10 family (Blumberg et al., 2001; Pestka et al., 2004), is expressed in



The Rockefeller University Press $30.00
J. Exp. Med. Vol. 208 No. 9 1849-1861
www.jem.org/cgi/doi/10.1084/jem.20102234

monocytes, epithelial cells, and endothelial cells. IL-20 acts on multiple cell types by activating a heterodimer receptor complex of either IL-20R1–IL-20R2 or IL-22R1–IL-20R2 (Dumoutier et al., 2001). It is involved in various inflammatory diseases (Wei et al., 2006), such as psoriasis (Blumberg et al., 2001; Wei et al., 2005; Sa et al., 2007), RA (Hsu et al., 2006), atherosclerosis (Caligiuri et al., 2006; Chen et al., 2006), ischemic stroke (Chen and Chang, 2009), and renal failure (Li et al., 2008). IL-20 is regulated by hypoxia and inflammatory stimuli such as IL-1β and LPS (Otkjaer et al., 2007; Chen and Chang, 2009). IL-20 has recently been reported to regulate angiogenesis (Heuzé-Vourc'h et al., 2005; Hsieh et al., 2006; Tritsaris et al., 2007). IL-20 induces synovial fibroblasts to secrete MCP-1, IL-6, and IL-8, and it acts as a proinflammatory cytokine (Hsu et al., 2006).

We previously (Hsu et al., 2006) showed that IL-20 is involved in RA and its soluble receptor of IL-20R1 blocked IL-20, which reduced the severity of collagen-induced arthritis (CIA). Therefore, IL-20 is a promoting factor during the progression of RA. However, little is known about the function of IL-20 in bone resorption or about the function of IL-20 in RANKL-RANK signaling-mediated osteoclastogenesis. Therefore, we explored the effect of anti–IL-20 monoclonal antibody 7E on osteoclast differentiation and its therapeutic potential to protect against osteoporotic bone loss.

## RESULTS

### Higher serum IL-20 in patients with osteopenia and osteoporosis

IL-20 is involved in the progression of RA, and IL-20R1 soluble receptor blocked IL-20 and protected against bone destruction in a CIA animal model (Hsu et al., 2006). Little is known, however, about the pathophysiology of IL-20 in osteoporotic bone destruction. Therefore, we examined whether IL-20 was involved in the pathogenesis of osteoporosis. We analyzed the IL-20 serum levels in the patients with osteopenia and osteoporosis and compared them with those of healthy controls. 33 healthy women (age range: 41–60 yr old), 62 women with osteopenia (age range: 41–67 yr old), and 37 women with osteoporosis (age range: 40–81 yr old) were included in the analysis (Table S1). The serum IL-20 concentration in osteopenia and osteoporosis patients was significantly higher than in healthy controls (Fig. 1 A). The median levels of serum IL-20 in the healthy controls, osteopenia, and osteoporosis patients were 15.38 pg/ml (25–75th percentiles, 0–109.3 pg/ml), 209.5 pg/ml (25–75th percentiles, 0–453.5 pg/ml), and 181.3 pg/ml (25–75th percentiles, 20.41–593.3 pg/ml), respectively.

### 7E protected ovariectomized (OVX) mice against bone destruction and increased bone mineral density (BMD)

Osteopenia and osteoporosis patients had more IL-20 in their serum than did healthy controls, which suggested that the IL-20 might be involved in the pathogenesis of bone loss. We generated a mouse anti–human IL-20 monoclonal antibody 7E and demonstrated its therapeutic potential because it could inhibit IL-20 in vitro and in vivo (Hsu et al., 2006; Chen and Chang, 2009). We also analyzed all members of the IL-10 family (IL-10, -19, -20, -22, -24, and -26) to confirm the specificity of 7E using ELISA. Only IL-20 was recognized by 7E (Fig. S1, A and B). Thus, we generated an ovariectomy-induced osteoporosis mouse model to investigate how IL-20 was involved in osteoclastogenesis and to examine the therapeutic effect of 7E on osteoporotic bone loss.

The serum level of IL-20 was up-regulated in the OVX mice but reduced in OVX mice treated with 7E (Fig. 1 B). Micro-computed tomography (micro-CT) scans of the mice tibia showed less bone loss in OVX mice treated with 7E (Fig. 1 C). It also showed a significant dose–response increase in the BMD of tibia in those mice (Fig. 1 D). Lower osteoclast numbers (N.Oc/BS) and smaller osteoclast areas of bone surface (Oc.S/BS) were observed in 7E-treated OVX mice (Fig. 1, E and F). Measurements of serum levels of C-terminal telopeptide of collagen (CTX), a marker of bone resorption, confirmed that OVX mice had higher bone resorption than did sham control mice. 7E-treated OVX mice had lower serum CTX than did mIgG-treated OVX control mice (Fig. S1 C). Bone histomorphometric analysis showed that the OVX procedure caused a significantly lower bone volume (Fig. S1 E, BV/TV), trabecular bone thickness (Fig. S1 G, Tb.Th), and trabecular number (Fig. S1 F, Tb.N.) in mIgG-treated OVX mice than in 7E-treated OVX mice. 7E-treated OVX mice also showed lower trabecular separation (Fig. S1 H, Tb.Sp) than mIgG-treated OVX control mice.

### 7E inhibited osteoclast differentiation

Bone formation is tightly regulated by cross talk between osteoblasts and osteoclasts. Unbalanced osteoclastogenesis causes bone loss in osteoporosis (Ross and Teitelbaum, 2005; Takayanagi et al., 2005). Thus, we wanted to determine whether 7E inhibits the differentiation of osteoclasts, thereby protecting OVX mice against bone loss. Osteoclast precursor cells were prepared from bone marrow–derived hematopoietic stem cells (HSCs), and both M-CSF and soluble (s) RANKL were added to the culture to drive osteoclast differentiation. We used two culture protocols to analyze the effect of 7E on osteoclast differentiation in the early and later stages of osteoclastogenesis. M-CSF–derived osteoclast precursor cells were cultured with 40 ng/ml of mouse M-CSF, 100 ng/ml sRANKL, and 2 μg/ml 7E for 6 d. TRAP staining was used to quantify the number of differentiated osteoclasts. 25 ng/ml TNF was a positive control for osteoclast differentiation. There were significantly fewer $TRAP^+$ osteoclasts in the 7E-treated group than in the mIgG-treated group (Fig. 2, A and B). We found almost no $TRAP^+$ osteoclasts in the 7E-treated group. To clarify whether 7E affected osteoclast differentiation in early or later stages, or both, we first incubated the HSCs with 7E or mIgG for 1 h and then added M-CSF for another 40 h. The cells were washed and then cultured in medium containing M-CSF and sRANKL without 7E for 8 d. Early incubation with 7E efficiently inhibited osteoclast differentiation (Fig. 2, C and D). Thus, 7E blocked both the

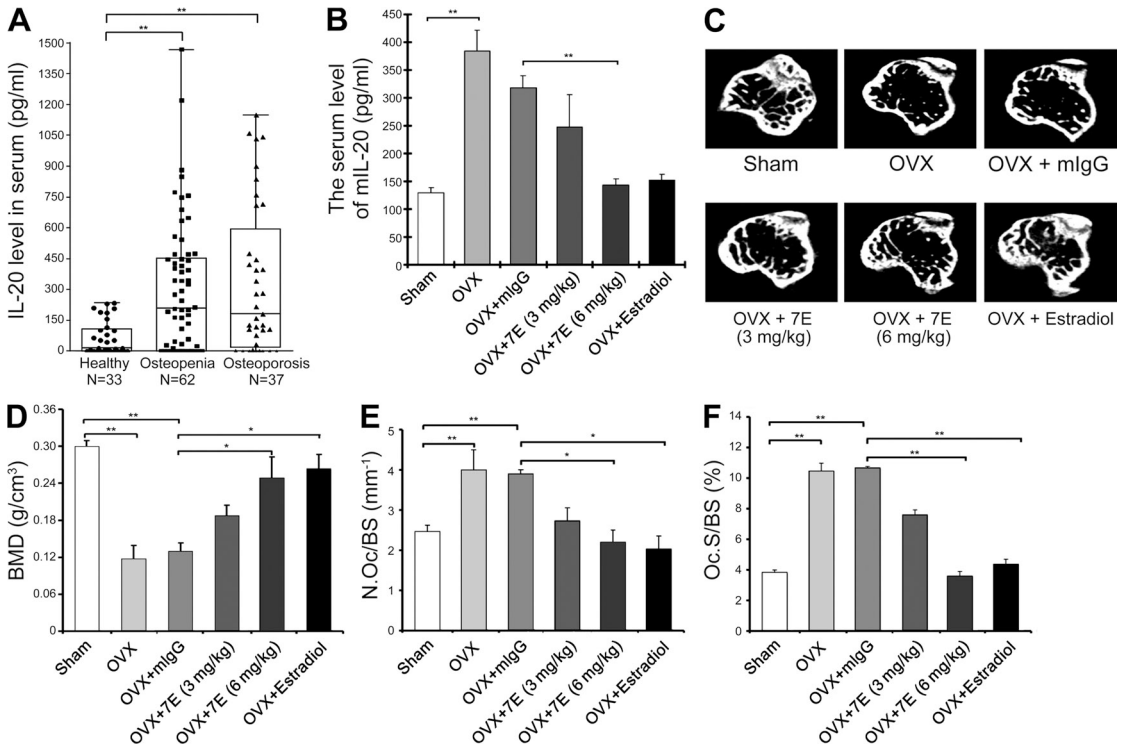


**Figure 1. A higher serum level of IL-20 was detected in osteopenia and osteoporosis patients.** (A) Level of IL-20 in serum from 33 healthy women, 62 women with osteopenia, and 37 women with osteoporosis was analyzed. Median levels of IL-20 were 15.38 pg/ml in healthy controls, 209.5 pg/ml in osteopenia patients, and 181.3 pg/ml in osteoporosis patients. Each box represents the 25–75th percentiles. Lines outside the boxes represent the 10th and 90th percentiles, and lines inside the boxes represent the median. Data are representative of three independent experiments. **, $P < 0.01$. (B) Serum levels of IL-20 in Sham or OVX mice treated with 3 or 6 mg/kg 7E, control Ab (mIgG), or 10 µg/kg 17β-estradiol. The treatment began 1 wk after surgery and the treatment was given every 3 d for 2 mo. Values are means ± SD. Data are representative of three independent experiments. **, $P < 0.01$. (C) Representative figures of micro-CT analysis of the right tibia of mice 2 mo after OVX ($n = 5$ or 6) or sham surgery ($n = 5$), followed by no treatment (OVX, $n = 5$), 10 µg 17β-estradiol/kg/d ($n = 6$), 6 mg mIgG/kg/3 d ($n = 6$), 3 mg 7E/kg/3 d ($n = 5$), or 6 mg 7E/kg/3 d ($n = 5$). Data are representative of three independent experiments. (D) BMD in the tibias of each experimental group. Values are means ± SD. Data are representative of three independent experiments. *, $P < 0.05$; **, $P < 0.01$. (E and F) Osteoclast numbers (E) and osteoclast areas (F) per bone surface in TRAP-stained sections. N.Oc/BS, number of osteoclasts per bone surface; Oc.S/BS, osteoclast surface per bone surface. Values are means ± SD. Data are representative of three independent experiments. *, $P < 0.05$; **, $P < 0.01$.

early and later stages of osteoclast differentiation. Furthermore, 7E markedly down-regulated the transcripts of RANK and osteoclast differentiation markers such as c-Fos, cathepsin K, NFATc1, and TRAP in the in vitro osteoclast differentiation system (Fig. 2, E–I). TNF also increased osteoclast formation. We therefore analyzed whether IL-20 directly induced osteoclast differentiation or indirectly promoted osteoclast differentiation by inducing TNF expression. Although TNF induced more osteoclast formation, 7E potently inhibited osteoclast formation in the presence of TNF, which suggested that the endogenous secretion of IL-20 by osteoclast precursor cells independently promotes osteoclast formation (Fig. 2 J).

### M-CSF up-regulated IL-20 in HSCs

7E blocked the differentiation of osteoclasts from M-CSF–derived osteoclast precursor cells (Fig. 2). We hypothesized that HSCs or osteoclast precursor cells expressed IL-20, which then acted as an autocrine mediator of osteoclastogenesis. To test this possibility, we examined IL-20 expression in the bone marrow–derived HSCs that had been cultured overnight and then treated with M-CSF for 6 h. RT quantitative (Q) PCR showed that IL-20 mRNA was higher in M-CSF–treated HSCs than in controls (Fig. 3 A), which was evidence that M-CSF caused endogenous IL-20 expression. In addition, three subunits of IL-20 receptor were expressed in the M-CSF–treated osteoclast precursor cells (Fig. 3 A) and mature osteoclasts (Fig. 3 B). These results suggested that IL-20 acted in an autocrine manner on the HSC-derived osteoclast precursor cells.

### IL-20 induced RANK expression in M-CSF–derived osteoclast precursor cells

The RANKL-RANK signal is critical for osteoclast differentiation (Wada et al., 2006). RANK is expressed on the surface of osteoclast precursor cells. To investigate whether IL-20 increases osteoclast differentiation by increasing RANKL-RANK signaling, we analyzed RANK expression in M-CSF–derived osteoclast precursor cells from bone marrow cells. The cytoplasmic RANK mRNA (Fig. 3 C) and surface expression of RANK protein (Fig. 3 D) were up-regulated in IL-20–treated osteoclast precursor cells. Consistent with its inhibition of osteoclast

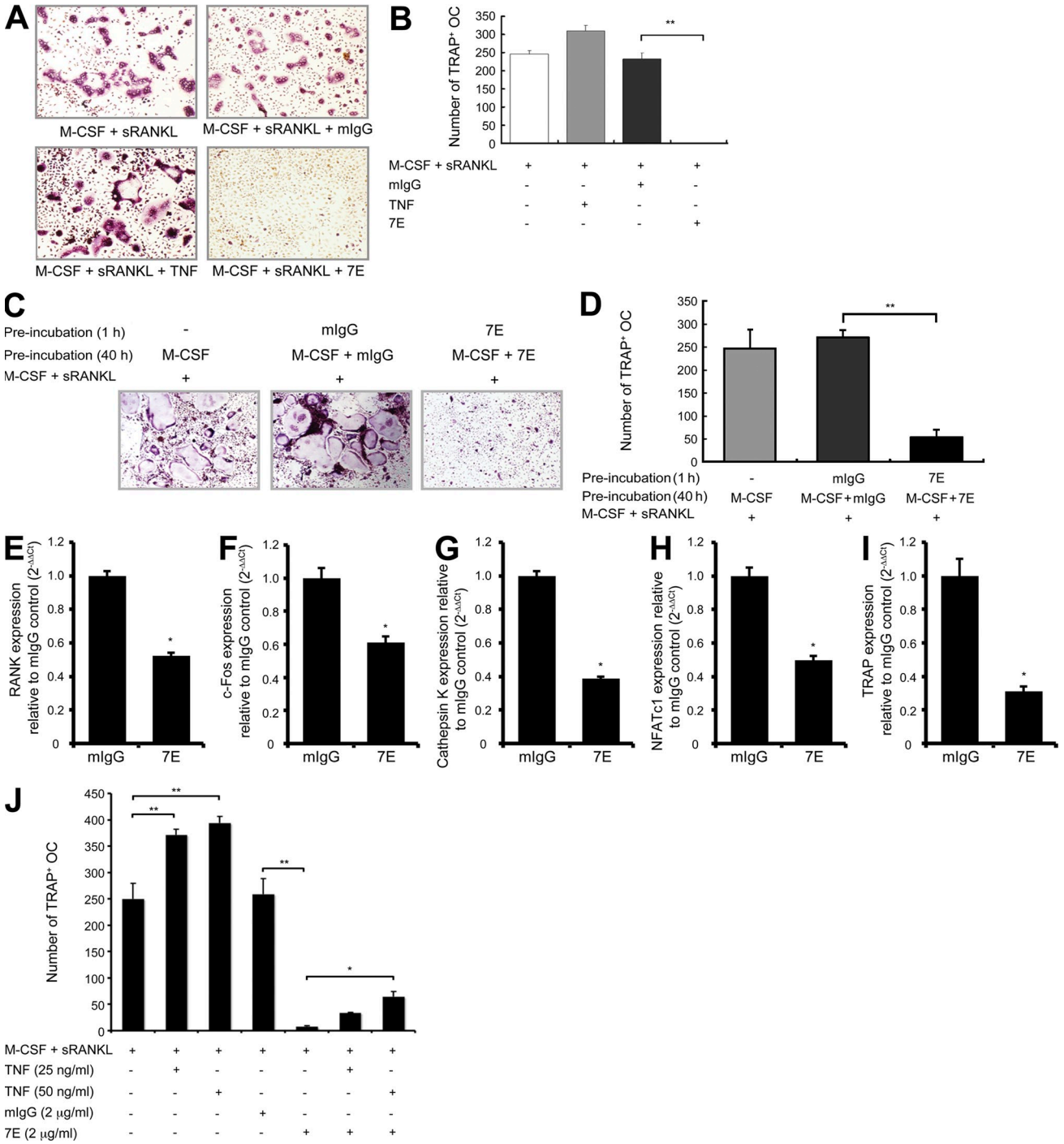


**Figure 2. Anti–IL-20 monoclonal antibody 7E inhibited osteoclast differentiation.** Bone marrow cells from the tibias of mice were incubated for 12 h. Later, nonadherent cells were collected and cultured with 30 ng/ml M-CSF. After 48 h, M-CSF–derived osteoclast precursor cells were treated with 2 μg/ml 7E, 2 μg/ml mIgG or 25 ng/ml TNF in α-MEM with 40 ng/ml M-CSF and 100 ng/ml sRANKL until the end of the experiment. (A) Representative TRAP staining of osteoclasts. Data are representative of three independent experiments. (B) Quantitation of TRAP+ osteoclasts per well. Values are means ± SD of 12 wells. Data are representative of three independent experiments. **, $P < 0.01$. (C) Representative TRAP staining of osteoclasts. Osteoclasts were cultured as described, but 7E was included during the first 2 d of culture in M-CSF. (D) Quantitation of TRAP+ osteoclasts per well. Values are means ± SD of 12 wells. Data are representative of three independent experiments. **, $P < 0.01$. (E–I) Osteoclast precursor cells were treated with M-CSF and sRANKL combined with 2 μg/ml 7E or 2 μg/ml of control IgG, mRNA was isolated, and the transcripts of RANK, c-Fos, cathepsin K, NFATc1, and TRAP were measured by RTQ-PCR at day 6 after culture. Data are the means ± SD of three independent experiments each performed in triplicates. *, $P < 0.05$. (J) Osteoclast precursor cells were treated with M-CSF and sRANKL combined with 25–50 ng/ml TNF and 2 μg/ml 7E or 2 μg/ml of control IgG. The number of TRAP+ osteoclasts per well is shown. Values are means ± SD of 12 wells. Data are representative of three independent experiments. *, $P < 0.05$; **, $P < 0.01$.

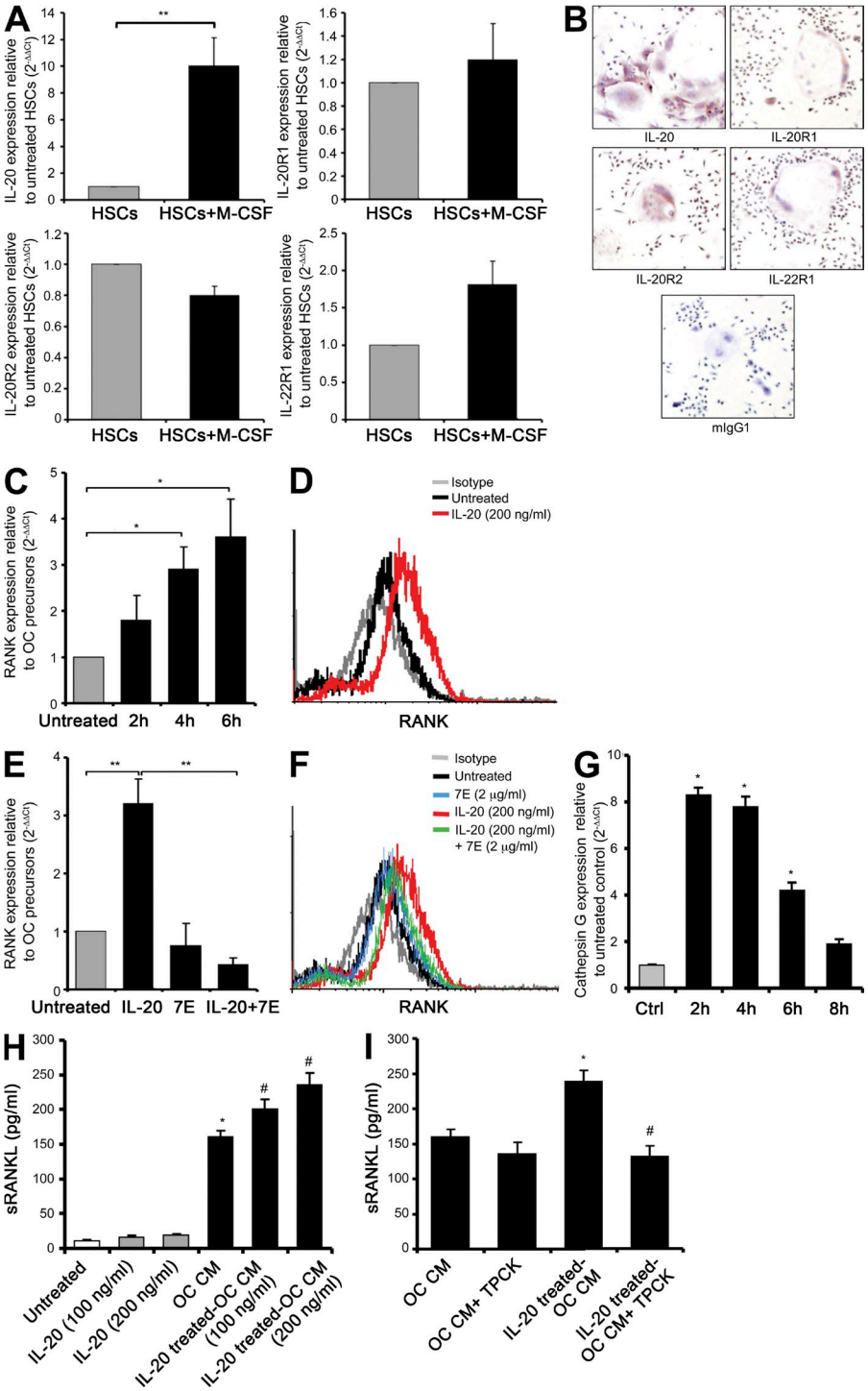


**Figure 3. Functions of IL-20 in osteoclasts.** (A) Bone marrow–derived HSCs were incubated with 50 ng/ml M-CSF for 6 h. mRNA was isolated and IL-20, IL-20R1, IL-20R2, and IL-22R1 mRNA expression was measured by RTQ-PCR. Values are means ± SD of 5 wells. Data are representative of three independent experiments. **, $P < 0.01$. (B) Mature osteoclasts were stained for expression of IL-20, IL-20R1, IL-20R2, and IL-22R1 protein or with a mouse IgG1 (mIgG1) isotype control. (C and E) M-CSF–derived osteoclast precursor cells were stimulated with 200 ng/ml IL-20 alone (C) or in combination with 2 μg/ml 7E (E) for the indicated times and RANK mRNA was measured by RTQ-PCR. Values are means ± SD of 5 wells. Data are representative of three independent experiments. *, $P < 0.05$; **, $P < 0.01$. (D and F) M-CSF–derived osteoclast precursor cells were cultured for 24 h with 200 ng/ml IL-20 alone (D) or in combination with 2 μg/ml 7E (F). Cells were scraped and then incubated for 30 min with anti–mouse PE-conjugated RANK antibody or isotype control antibody. Surface RANK expression was analyzed using flow cytometry. Data are representative of three independent experiments. (G) Mature osteoclasts were stimulated with 200 ng/ml IL-20 for the indicated times and cathepsin G mRNA was measured by RTQ-PCR. Values are means ± SD of 5 wells. Data are representative of three independent experiments. *, $P < 0.05$ versus untreated controls. (H) MC3T3-E1 cells were incubated with IL-20–treated OC CM or PBS-treated OC CM for 20 h, and the production of sRANKL was measured by ELISA. Data are the means ± SD of three independent experiments each performed in triplicates. *, $P < 0.05$ versus untreated controls; #, $P < 0.05$ versus OC CM. (I) Control or IL-20–treated OC CM was incubated with 10 μM of a cathepsin G–specific inhibitor (TPCK) for 1 h at 37°C before MC3T3-E1 culture for 20 h. sRANKL concentration in the final culture medium was determined by ELISA. Data are the means ± SD of three independent experiments each performed in triplicates. *, $P < 0.05$ versus OC CM; #, $P < 0.01$ versus IL-20–treated OC CM.

differentiation, 7E inhibited both the expression of RANK transcripts (Fig. 3 E) and the surface expression of RANK protein (Fig. 3 F). These results are evidence that IL-20 acts as an osteoclastogenic cytokine on osteoclast precursor cells.

### IL-20 induced cathepsin G expression in osteoclasts

Cathepsin G, highly expressed in osteoclasts, is capable of shedding the extracellular domain of RANKL from osteoblasts to generate active soluble RANKL and inducing the differentiation and activation of osteoclast precursors (Wilson et al., 2008). IL-20 induced the expression of cathepsin G in M-CSF–derived mature osteoclasts (Fig. 3 G). Therefore, we hypothesized that IL-20–treated osteoclasts produce a high level of cathepsin G and subsequently cleave membrane-bound RANKL to generate a soluble form of RANKL, which further stimulates osteoclast differentiation. To confirm this mechanism, we incubated osteoblastic MC3T3-E1 cells with IL-20–treated osteoclast

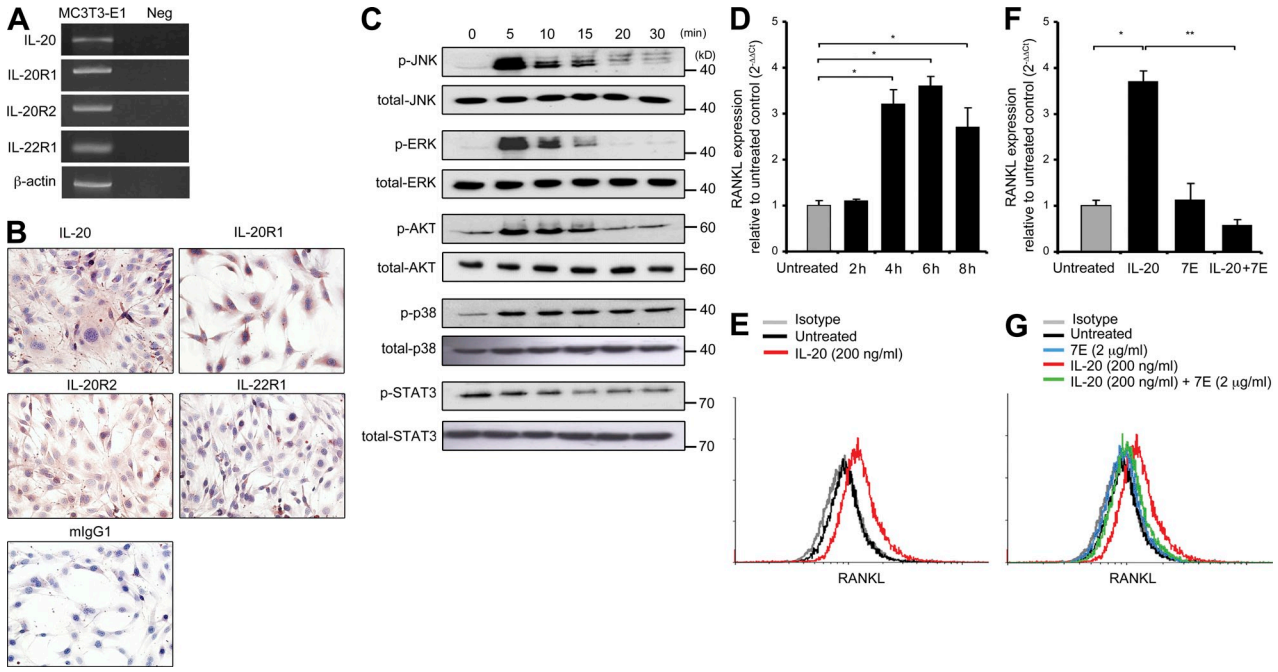


**Figure 4. Functions of IL-20 in osteoblastic MC3T3-E1 cells.** (A) The expression of IL-20 and its receptors in MC3T3-E1 cells was analyzed using RTQ-PCR. (B) MC3T3-E1 cells were stained for expression of IL-20, IL-20R1, IL-20R2, IL-22R1, or isotype control (mIgG1). (C) MC3T3-E1 cells were incubated with IL-20 for the indicated time periods, and cell lysates were analyzed by immunoblotting for the indicated protein. Data are representative of three independent experiments. (D and F) MC3T3-E1 cells were treated with 200 ng/ml IL-20 alone (D) or in combination with 2 μg/ml 7E (F) for the indicated times and RANKL mRNA was analyzed by RTQ-PCR. Values are means ± SD of 5 wells. Data are representative of three independent experiments. *, $P < 0.05$; **, $P < 0.01$. (E and G) MC3T3-E1 cells were cultured for 16 h with 200 ng/ml IL-20 alone (E) or in combination with 2 μg/ml 7E (G). Surface RANKL expression was analyzed using flow cytometry. Data are representative of three independent experiments.

conditioned medium (OC CM) for 20 h. ELISA assay showed that IL-20–treated OC CM cleaved a large amount of sRANKL derived from MC3T3-E1 cells (Fig. 3 H). We also directly treated MC3T3-E1 cells with IL-20 alone as a control. There were no differences in the amount of sRANKL in the media between the untreated and IL-20–treated MC3T3-E1 cells. To confirm that the cleavage of RANKL was cathepsin G dependent, we used a specific cathepsin G inhibitor (TPCK, 10 μM) to block the protease activity of cathepsin G. The result confirmed our hypothesis (Fig. 3 I). Therefore, IL-20 was also involved in osteoclastogenesis by inducing cathepsin G and modulating sRANKL production by osteoblast.

### IL-20 targeted osteoblasts and up-regulated RANKL expression

Increased RANKL expression in osteoblasts is also a key factor for osteoclastogenesis (Wada et al., 2006). We used RTQ-PCR (Fig. 4 A) and cytochemical staining (Fig. 4 B) to show that IL-20 and its receptor subunit were expressed in osteoblastic MC3T3-E1 cells. Phosphorylation of JNK, ERK, AKT, and p38 were detected in IL-20–treated MC3T3-E1 cells (Fig. 4 C), more evidence that IL-20 was endogenously expressed in osteoblasts and triggered signal transduction in them in an autocrine manner. To determine whether IL-20 contributes to osteoclastogenesis by inducing RANKL expression in osteoblasts, we incubated the MC3T3-E1 cells with IL-20 and analyzed RANKL expression using RTQ-PCR and flow cytometry. RANKL expression was time-dependently higher in IL-20–treated MC3T3-E1 cells than in untreated controls, and it peaked 6 h after treatment (Fig. 4 D). The surface expression of RANKL protein was also higher in IL-20–treated MC3T3-E1 cells (Fig. 4 E).

### 7E inhibited IL-20–induced RANKL expression in osteoblasts

RANKL expression was up-regulated in IL-20–treated MC3T3-E1 cells (Fig. 4, D and E). To confirm that 7E inhibits IL-20-induced RANKL expression, we co-treated the cells with IL-20 and 7E. RTQ-PCR detected almost no RANKL transcripts in co-treated cells (Fig. 4 F), and surface RANKL protein expression was lower in co-treated cells than in cells treated only with IL-20 (Fig. 4 G). These results indicated that IL-20 is an upstream activator of RANKL expression in osteoblasts and that 7E inhibits IL-20–induced RANKL expression. These in vitro results are evidence that IL-20 is an upstream mediator of RANKL and is involved in osteoclastogenesis.

### IL-20R1 deficiency inhibited osteoclast differentiation

IL-20 up-regulated RANK expression in osteoclast precursor cells and up-regulated RANKL expression in osteoblasts (Figs. 3 and 4). Our previous study (Hsu et al., 2006) showed

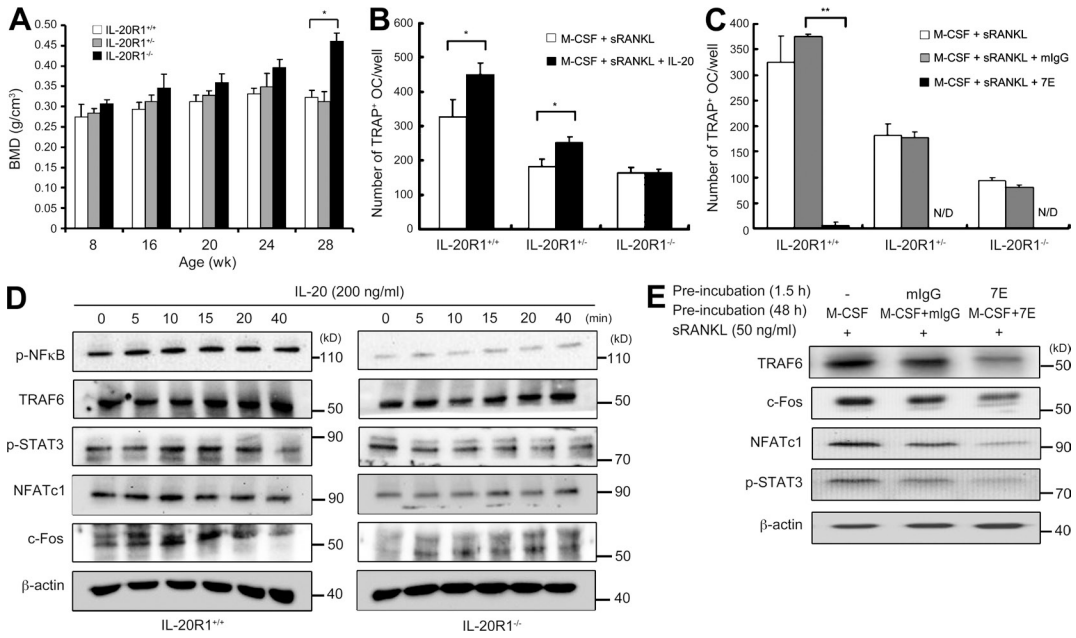


**Figure 5. IL-20R1 deficiency increased BMD in vivo and inhibited IL-20–induced osteoclast differentiation and signal transduction in vitro.** (A) BMD in the tibias of 28-wk-old IL-20R1 WT (+/+), heterozygote (+/−), and knockout (−/−) mice ($n$ = 5/group). Values are means ± SD of five mice. Data are representative of three independent experiments. *, $P < 0.05$. (B) M-CSF–derived osteoclast precursor cells from the indicated mice were treated with M-CSF and sRANKL combined with 200 ng/ml IL-20. Values are means ± SD of five mice. Data are representative of three independent experiments. *, $P < 0.05$. (C) M-CSF–derived osteoclast precursor cells from the indicated mice were treated with M-CSF and sRANKL combined with 2 µg/ml 7E or 2 µg/ml mIgG. Values are means ± SD of five mice. Data are representative of three independent experiments. **, $P < 0.01$. (D) M-CSF–derived osteoclast precursor cells from IL-20R1$^{+/+}$ and IL-20R1$^{-/-}$ mice were cultured with IL-20 for the indicated time periods, and the cell lysates were immunoblotted for the indicated protein. Data are representative of three independent experiments. (E) Bone marrow–derived HSCs from WT mice were incubated with 40 ng/ml M-CSF with 2 µg/ml 7E or 2 µg/ml of control mIgG for 48 h followed by 50 ng/ml sRANKL for 48 h. Cell lysates were immunoblotted for the indicated protein. Data are representative of three independent experiments.

that IL-20R1 was significantly up-regulated in CIA animal model and that treatment with the soluble receptor of IL-20R1 ameliorated the severity of CIA, which suggested that IL-20R1 is critical for IL-20 signaling. To confirm the critical involvement of IL-20 in osteoclastogenesis, we generated IL-20R1 knockout mice and analyzed the effect of IL-20R1 deficiency on IL-20–induced osteoclastogenesis. To generate IL-20R1 knockout mice, we first examined whether the deletion of exon 2 completely blocked the expression of IL-20R1. The deletion of exon 2 of IL-20R1 abolished the translation of IL-20R1-EGFP fusion protein, which showed that exon 2 is a target for IL-20R1 gene disruption (Fig. S2 A). To block IL-20R1 gene expression, we used homologous recombination to delete exon 2 (Fig. S2 B) and Southern blotting with the probe annealed to 3′ of the target sequence to verify the deletion of the IL-20R1 allele (Fig. S2 C). IL-20 binds to one of its two receptor complexes: IL-20R1–IL-20R2 and IL-20R2–IL-22R1. In the coimmunoprecipitation assay, the lysates of lung tissue from WT (+/+), heterozygote (+/−), and knockout (−/−) mice were incubated with His-tagged IL-20 and pulled down by anti-His antibody. The pulled-down pellet was analyzed using immunoblotting with antibodies against IL-20, IL-20R1, IL-20R2, and IL-22R1. No IL-20R1 protein was detected in the lung lysates from IL-20R1$^{-/-}$ mice (Fig. S2 D). To confirm that cells isolated from IL-20R1$^{-/-}$ mice did not have functional IL-20R1 protein, we used IL-19 to target the cells because IL-19 binds only to IL-20R1/IL-20R2. IL-19 induced IL-10 expression in PBMCs through the IL-20R1–IL-20R2 receptor complex (Jordan et al., 2005). We isolated the PBMCs from IL-20R1$^{+/+}$, IL-20R1$^{+/-}$, and IL-20R1$^{-/-}$ mice and then treated them with IL-19. IL-19–induced IL-10 expression was abolished in IL-20R1$^{-/-}$ PBMCs (Fig. S2 E), which confirmed that the IL-20R1 gene had been successfully deleted in IL-20R1$^{-/-}$ mice. The BMD in the tibias was significantly higher in IL-20R1$^{-/-}$ mice than in IL-20R1$^{+/+}$ mice when they reached the age of 28 wk (Fig. 5 A). Bone histomorphometric analysis showed that bone volume and trabecular bone thickness were also higher in IL-20R1$^{-/-}$ mice than in IL-20R1$^{+/+}$ mice (Fig. S3, A–D). We also analyzed the RANK and RANKL level in the proximal tibia of WT and IL-20R1$^{-/-}$ mice. RTQ-PCR revealed that both RANKL and RANK were down-regulated in IL-20R1$^{-/-}$ mice compared with WT mice (Fig. S3, E and F), demonstrating that IL-20 is involved in the regulation of the RANK-RANKL in vivo. Furthermore, the transcripts of RANK and osteoclast differentiation markers were analyzed in the in vitro osteoclast differentiation system. RANK and osteoclast differentiation markers such as c-Fos, cathepsin K, NFATc1, and TRAP were markedly down-regulated in IL20R1-deficient cells (Fig. S4, A–E).

In IL-20R1$^{+/+}$ mice, TRAP$^{+}$ osteoclasts were higher in M-CSF–derived osteoclast precursor cells treated with IL-20. In both IL-20R1$^{+/-}$ and IL-20R1$^{-/-}$ mice, however, the basal level of TRAP$^{+}$ osteoclasts was lower (Fig. 5 B). In addition, osteoclast differentiation was significantly inhibited in the IL-20R1$^{-/-}$ group treated with IL-20 (Fig. S4 F), which indicated that IL-20R1 signaling is critical for IL-20-mediated osteoclastogenesis. To examine the inhibitory effect of 7E on osteoclast differentiation, we compared the TRAP$^{+}$ osteoclasts derived from the IL-20R1$^{+/+}$, IL-20R1$^{+/-}$, and IL-20R1$^{-/-}$ osteoclast precursor cells. 7E completely blocked in vitro osteoclast differentiation in all three types of mice (Fig. 5 C), which confirmed the pivotal role of IL-20 in osteoclast differentiation and that 7E blocks osteoclastogenesis.

Furthermore, we performed the mixed co-cultures of osteoclasts and osteoblasts by reciprocal combinations of these two cell populations from WT and IL-20R1$^{-/-}$ mice to determine the relative contribution of each to osteoclastogenesis. IL-20 is critical to both osteoclast and osteoblast because IL-20R1 deficiency impaired osteoclast differentiation in the mixed co-cultures of both WT osteoblast/IL-20R1$^{-/-}$ osteoclast precursors and IL-20R1$^{-/-}$ osteoblast/WT osteoclast precursors (Fig. S5 A). The co-cultures of IL-20R1$^{-/-}$ osteoclast precursors with WT osteoblast did not show as much impairment of osteoclast differentiation as the osteoblast-free system (Fig. 5 B) in which M-CSF and sRANKL were added to IL-20R1$^{-/-}$ osteoclast precursors to replace osteoblast. Because IL-20 was endogenously expressed in mature osteoblast, we hypothesized that WT osteoblast, in response to IL-20, may secrete TNF which enhanced osteoclast differentiation independent of IL-20R1 signaling. To test this possibility, we compared the induction of TNF transcript in response to IL-20 in mature osteoblast from WT and IL-20R1$^{-/-}$ mice. IL-20 up-regulated TNF expression in WT osteoblasts but not in IL-20R1-deficient osteoblasts (Fig. S5 B). The observation indicated that IL-20R1 deficiency affected the function of osteoblasts. In addition, the WT osteoblasts produced more RANKL in response to IL-20 than IL-20R1–deficient osteoblasts did (Fig. S5 C), which may result in more osteoclast differentiation from WT osteoblast/IL-20R1$^{-/-}$ osteoclast precursor co-culture than from IL-20R1$^{-/-}$ osteoblast/WT osteoclast precursor co-culture.

### IL-20 promoted osteoclastogenic signal transduction in M-CSF–derived osteoclast precursor cells

RANKL–RANK signaling-mediated NFATc1 activation is pivotal for osteoclast differentiation. To determine whether IL-20 signaling contributes to the alteration of osteoclastogenic signaling, we treated M-CSF–derived osteoclast precursor cells with IL-20 and found that IL-20 promoted the activation of NF-κB, TRAF6, STAT3, NFATc1, and c-Fos (Fig. 5 D). The activation of IL-20–induced osteoclastogenic signals was lower in IL-20R1$^{-/-}$ than in IL-20R1$^{+/+}$ mouse-derived osteoclast precursor cells. In addition, 7E almost totally

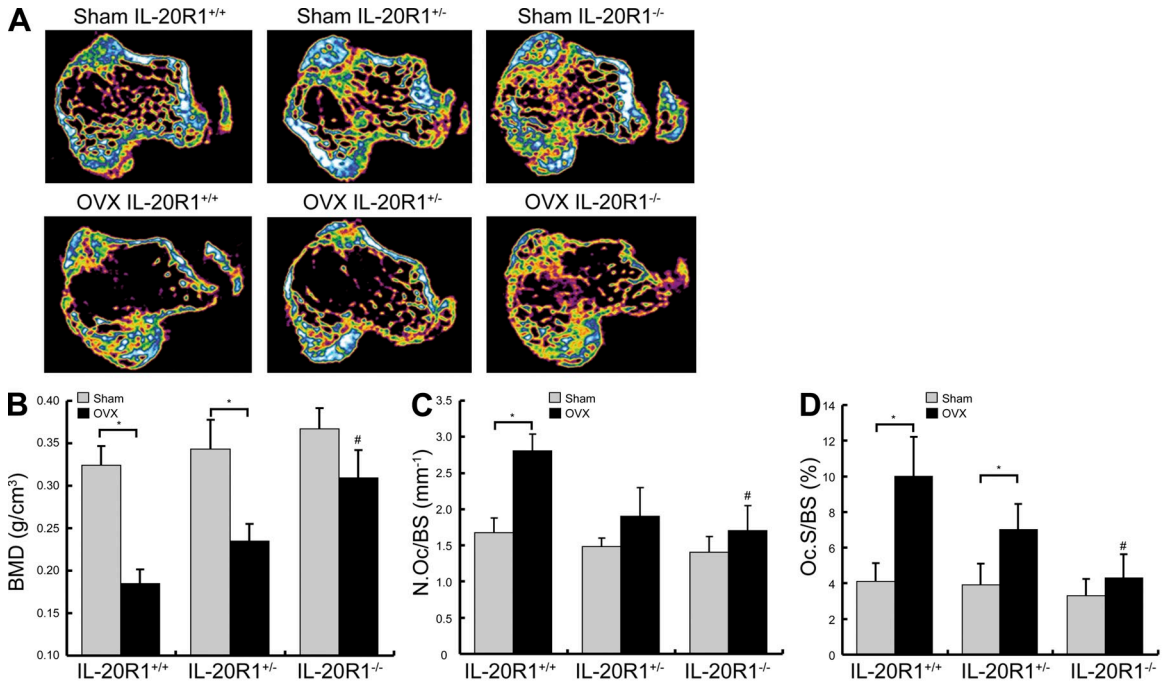


**Figure 6. IL-20R1 deficiency protected mice from OVX-induced bone loss.** (A) Micro-CT analysis of the right tibias of IL-20R1$^{+/+}$, IL-20R1$^{+/-}$, and IL-20R1$^{-/-}$ mice 2 mo after OVX treatment ($n$ = 5/group). Data are representative of three independent experiments. (B) BMD in the tibias of OVX mice. Values are means ± SD of five mice. Data are representative of three independent experiments. (C and D) The number of osteoclasts (C) and osteoclast areas (D) per bone surface in TRAP-stained sections. N.Oc/BS, number of osteoclasts per bone surface; Oc.S/BS, osteoclast surface per bone surface ($n$ = 5). Values are means ± SD of five mice. Data are representative of three independent experiments. *, P < 0.05 versus corresponding sham-operated mice; #, P < 0.05 versus OVX-IL-20R1$^{+/+}$ mice.

prevented the RANKL-induced activation of TRAF6, c-Fos, NFATc1, and STAT3, which suggested that IL-20 had triggered the osteoclastogenic signals and was a costimulatory factor for osteoclastogenesis (Fig. 5 E).

### IL-20R1 deficiency protected OVX mice against bone loss

To confirm the in vivo role of IL-20 in osteoclast differentiation, we used micro-CT analysis, in a model of OVX-induced osteoporosis, to investigate whether IL-20R1 receptor signaling was crucial for controlling BMD (Fig. 6 A). OVX induced a significant loss of BMD and increased N.Oc/BS and Oc.S/BS in IL-20R1$^{+/+}$ mice but not in IL-20R1$^{-/-}$ mice (Fig. 6, B–D). Measurements of serum CTX confirmed that OVX increased bone resorption in IL-20R1$^{+/+}$ mice but not in IL-20R1$^{-/-}$ mice (Fig. S6 A). OVX induced bone loss in IL-20R1$^{+/+}$ mice. However, no significant bone loss occurred in OVX-IL-20R1$^{-/-}$ mice. Parameters of trabecular structure were also differentially affected by OVX in IL-20R1$^{+/+}$ and IL-20R1$^{-/-}$ mice because bone volume, trabecular bone thickness, trabecular number, and trabecular separation were more substantially deteriorated by OVX in IL-20R1$^{+/+}$ than in IL-20R1$^{-/-}$ mice (Fig. S6, C–F). Collectively, these results showed that IL-20 was important for osteoclast differentiation and that IL-20/IL-20R1 signaling was critical for regulating BMD during metabolic bone disease.

## DISCUSSION

We showed that IL-20 was higher both in patients with osteoporotic bone loss and in OVX mice. IL-20 stimulates osteoclast differentiation and blocking IL-20 activity with the specific anti–IL-20 monoclonal antibody 7E has therapeutic potential for osteoporotic bone loss. The conventional wisdom is that M-CSF and RANKL are both necessary and sufficient for osteoclast differentiation. However, we showed that IL-20 endogenously secreted from HSCs is also essential for osteoclast differentiation; our evidence is that 7E completely blocked osteoclast differentiation in the presence of M-CSF and RANKL. In the correlation between IL-20 and the RANKL–RANK axis, we found that IL-20 up-regulated RANK expression on osteoclast precursors derived from bone marrow cells. In addition, IL-20 caused RANKL expression on osteoblasts. Even though TNF also promoted osteoclast formation, 7E potently inhibited osteoclast differentiation in the presence of TNF, which suggested that IL-20 may act independently on osteoclast differentiation. Treatment with 7E prevented IL-20 from inducing RANK and RANKL expression. IL-20–induced osteoclast differentiation was inhibited in IL-20R1$^{-/-}$ mouse-derived osteoclast precursor cells. We therefore conclude that IL-20R1 is important in IL-20–mediated osteoclastogenesis, and that IL-20 is an upstream activator of RANKL-RANK signaling. IL-20 is pivotal in osteoclast differentiation because it targeted not only osteoclast precursor cells but also osteoblasts.

Osteoclasts originate from hematopoietic progenitor cells, probably from CFU granulocyte-macrophages (GMs; Menaa et al., 2000). CFU-GMs are different from multipotential progenitor cells, CFU-GEMMs. One study (Liu et al., 2003) showed that IL-20 specifically promoted the in vitro and in vivo proliferation of CFU-GEMMs. We showed that M-CSF up-regulated IL-20 in osteoclast precursor cells. IL-20, in an autocrine manner, targeted osteoclast precursor cells and increased the expression of RANK. In addition, IL-20 activated osteoclastogenic signaling and 7E inhibited the activation of NFATc1, the master regulator for osteoclast differentiation. Therefore, we hypothesize that IL-20 contributes to osteoclastogenesis by promoting both the survival and the expansion of osteoclast precursor cells and increasing RANKL-induced activity. In the osteoclast differentiation assay, 7E blocked both early and later stage differentiation, which supports our hypothesis.

Cathepsin G is also a chemoattractant for osteoclast precursors by proteolytically activating PAR-1 (Wilson et al., 2009). In the present study, IL-20 up-regulated the expression of cathepsin G in osteoclasts, which dose-dependently induced the cleavage of RANKL from the surface membrane of osteoblasts. Therefore, we speculate that IL-20 acts on osteoclasts to produce a large amount of cathepsin G in bone microenvironment. The IL-20–induced cathepsin G, in turn, recruits more osteoclast precursors that differentiate into mature osteoclasts and produce more cathepsin G, which leads to the generation of sRANKL.

The RANKL–RANK signaling mechanism is one pathway of osteoclast formation and activity (Kong et al., 1999; Li et al., 2000). We found that IL-20 increased RANKL mRNA and RANKL protein expression in osteoblasts, which suggested that IL-20 is an upstream regulator for RANKL expression. RANKL expression is also up-regulated in many malignant tumor cells, and is involved in cancer-associated bone destruction, tumor metastasis, and tumor-induced osteolysis (Park et al., 2007; Wilson et al., 2008). We previously (Hsing et al., 2006) showed that IL-20 is expressed in squamous cell carcinoma of the skin, tongue, esophagus, and lung. However, the association of IL-20 with tumor progression and metastasis has not been clarified. It is therefore necessary to explore the effects of 7E on cancer-associated bone metastasis and bone erosion.

Soluble RANK antagonists and RANKL inhibitors such as osteoprotegerin and anti-RANKL antibody are inhibitors of bone resorption in clinical studies, presumably because of their effects on osteoclasts. One therapeutic drug to treat osteoporosis is denosumab, an anti-RANKL antibody (Kostenuik, 2005; McClung, 2006). Our results also showed that 7E protected OVX mice against osteoporotic bone loss and increased their BMD. In the in vitro assay, we showed that 7E reduced not only the number of TRAP$^{+}$ osteoclasts, but also the expression of RANK in M-CSF–derived osteoclast precursor cells and of RANKL in osteoblasts. In addition, 7E almost totally prevented the RANKL-induced activation of TRAF6, c-Fos, NFATc1, and STAT3 because it down-regulated RANK expression in osteoclast precursors. Thus, 7E shows promise as a therapeutic drug for protection against bone destruction.

BMD is regulated by osteoclastogenic and osteoblastogenic activity (Walsh et al., 2005). IL-20R1 deficiency protected

mice from OVX-induced bone loss. This finding is consistent with our finding that serum IL-20 levels were higher in patients with osteopenia and osteoporosis than in healthy controls. This suggested that the osteoclastogenic activity of IL-20 might be activated only during pathological conditions such as estrogen deficiency or OVX-induced osteoporosis. To prove this, we treated healthy WT mice with 7E and found that it had no significant effect on their BMD compared with untreated mice. In addition, there was no significant difference in serum IL-20 levels between sham-operated mice treated with PBS and those treated with 7E, which indicated that serum IL-20 antibody from 7E treatment did not interfere with the ELISA analysis of IL-20 in 7E-treated OVX mice (unpublished data). Moreover, we still observed some in vitro osteoclast differentiation from osteoclast precursor cells of IL-20R1$^{-/-}$ mice. This may be attributable to the alternative IL-20R2–IL-22R1 receptor complex signaling. Expression of all the three receptor subunits on osteoclast precursor cells suggested this possibility. In vitro osteoclast differentiation was inhibited in osteoclast precursor cells derived from IL-20R1$^{-/-}$ mice with no effect of addition of IL-20. We hypothesize that the response threshold of IL-20 in IL-20R1$^{-/-}$ mice is much higher than in WT mice because of different receptor complex signaling. No significant difference in BMD was observed in the 8-wk-old IL-20R1$^{+/+}$, IL-20R1$^{+/-}$, and IL-20R1$^{-/-}$ mice. However, IL-20R1$^{-/-}$ mice had significantly higher BMD than did IL-20R1$^{+/+}$ mice when they reached the age of 28 wk. This difference raised the possibility that an age-related estrogen deficiency might affect IL-20 levels, the activity of which was inhibited in IL-20R1$^{-/-}$ mice. Additional studies are needed to explore the detailed molecular mechanism of estrogen's regulation of IL-20. The intercross co-cultures of osteoclast precursors with osteoblastic cells from WT and IL-20R1$^{-/-}$ mice demonstrated that the deficiency of IL-20R1 affected both osteoclast precursors and osteoblasts that impaired osteoclast differentiation. The co-cultures of IL-20R1$^{-/-}$ osteoclast precursors with WT osteoblastic cells did not show as much impairment of osteoclast differentiation as the osteoblast-free system (Fig. 5 B). This may be attributed to IL-20–induced TNF production in the WT osteoblasts. Thus, IL-20 and IL-20R1 signaling are crucial not only in osteoclast differentiation, but also in the function of osteoblast. These findings support the hypothesis that IL-20 produced by osteoblasts and osteoclasts stimulate IL-20R1 signaling, which mediates the cross talk between osteoclasts and osteoblasts and regulates the bone remodeling. Furthermore, whether IL-20 is also involved in osteoblast differentiation is not well understood. It is necessary to further investigate the mechanism that IL-20 uses to maintain the balance between osteoclastogenesis and osteoblastogenesis in metabolic bone destruction and inflammatory bone diseases.

In summary, our findings provide evidence that IL-20 is an osteoclastogenic cytokine that up-regulates RANK on osteoclast precursor cells and RANKL on osteoblasts and affects the functions of both cells. We identified a pivotal role of IL-20 in osteoclast differentiation, and we conclude that using 7E to inhibit IL-20 is a potential therapeutic strategy for protecting against osteoporotic bone loss.

## MATERIALS AND METHODS

**Patients.** 243 women (age range: 40–84 yr old) participating in a community-based chronic disease prevention study conducted from 2008 to 2009 by the Department of Family Medicine, National Cheng Kung University Hospital, were recruited for this study. Individuals with known metabolic bone diseases, taking any medications likely to influence BMD, who were bedridden, using steroids, alcohol dependent, or with a history of hypertension, diabetes mellitus, arthrosclerosis, renal disease, or cancer were excluded from this study. BMD for all study participants was determined using dual energy x-ray absorptiometry (DXA) of the lumbar spine, hip, and femoral neck. According to World Health Organization criteria, the participants were categorized into three groups based on the DXA results: (1) normal BMD ($T \leq -1$); (2) osteopenia ($-2.5 \leq T \leq -1$); and (3) osteoporosis ($T \leq -2.5$). Written informed consent was obtained and the study was approved by the Ethics Committee of National Cheng Kung University Hospital. Blood samples were collected and serum was prepared by nurses according to standard procedures. Blood was centrifuged (2,000 rpm for 10 min at 4°C), and serum was collected. All samples were stored at −80°C until used. Levels of IL-20 in the serum of the participants were determined using a human IL-20 ELISA kit (PeproTech) according to the manufacturer's instructions.

**Ovariectomy-induced bone loss model and treatments.** All animal experiments were conducted according to the protocols based on the National Institutes of Health standards and guidelines for the care and use of experimental animals. The research procedures were approved by the Animal Ethics Committee of National Cheng Kung University in Taiwan. 14-wk-old female BALB/c mice under general anesthesia (50 mg pentobarbital/kg body weight; Sigma-Aldrich) were OVX or sham operated (Sham Controls). The experiments began 1 wk after surgery and the mice were divided into six groups: sham controls ($n = 5$), OVX mice without treatment ($n = 5$), and OVX mice treated with 10 µg 17β-estradiol/kg/d ($n = 6$; Sigma-Aldrich), 6 mg mIgG/kg/3 d ($n = 6$; Millipore), 3 mg 7E/kg/3 d ($n = 5$), or 6 mg 7E/kg/3 d ($n = 5$). All the mice were given an overdose of pentobarbital 2 mo after the treatments had begun, and their tibias were aseptically collected, cleaned of adherent soft tissue, and analyzed with micro-CT scanning. Blood was centrifuged at 2,000 rpm for 10 min at 4°C, and serum was collected. Levels of IL-20 in the serum were determined using an IL-20 ELISA kit according to the manufacturer's instructions. To calculate the number of osteoclasts on the bone surface, the tibias were collected and frozen sectioned for TRAP staining 3 wk after the first treatment.

**Micro-CT.** The tibia metaphyses were analyzed in vivo on a micro-CT (1076; SkyScan) with a high resolution low-dose x-ray scanner. BMD, a three-dimensional bone characteristic parameter, was analyzed in 50 consecutive slices. Trabecular bone volume (BV/TV), trabecular bone thickness (Tb.Th), trabecular number (Tb.N.), and trabecular separation (Tb.Sp) were measured using the software developed for bone histomorphometry (CT-analyzer software; SkyScan).

**RTQ-PCR.** Total mRNA was isolated. Reverse transcription was done with reverse transcriptase according to the manufacturer's protocol (Takara Bio Inc). IL-20, IL-20R1, IL-20R2, IL-22R1, RANK, RANKL, cathepsin G, cathepsin K, c-Fos, TRAP, NFATc1, and TNF expression was then amplified on a thermo cycler (LC 480; Roche), with SYBR green (Roche) as the interaction agent. Quantification analysis of mRNA was normalized with mGAPDH as the housekeeping gene. Relative multiples of change in mRNA expression was determined by calculating $2^{-\Delta\Delta Ct}$.

**In vitro osteoclastogenesis assay.** Bone marrow cells from the tibias of WT C57BL/6, IL-20R1$^{+/-}$, or IL-20R1$^{-/-}$ mice were incubated for 12 h at 37°C in 5% $CO_2$. Later, nonadherent cells were collected and seeded in 24-well plates ($2 \times 10^6$ cells per well) and cultured in the same medium

supplemented with 30 ng/ml of recombinant mouse M-CSF (PeproTech). After 48 h, M-CSF–derived osteoclast precursor cells were cultured with 40 ng/ml of mouse M-CSF and 100 ng/ml sRANKL (PeproTech) until the end of the experiment. To analyze the effect of 7E in the early stage of osteoclast differentiation, bone marrow cells were cultured for 12 h. Nonadherent cells were seeded in 24-well plates ($2 \times 10^6$ cells per well) and cultured in α-MEM containing 2 μg/ml 7E or 2 μg/ml mIgG, after which 40 ng/ml M-CSF was added. After 40 h, the treatment ended, and the cells were washed with serum-free culture medium and then incubated with 40 ng/ml M-CSF and 100 ng/ml sRANKL for 8 d. In another experiment, to analyze the effect of 7E in the later stage of osteoclast differentiation, M-CSF–derived osteoclast precursor cells were treated with 2 μg/ml 7E or 2 μg/ml mIgG in α-MEM with M-CSF and sRANKL for 6 d. To assay the effects of TNF and IL-20 on osteoclast differentiation, M-CSF–derived osteoclast precursor cells were treated with 25–50 ng/ml of mouse TNF (R&D Systems) plus 2 μg/ml 7E in α-MEM with M-CSF and sRANKL for 8 d. The culture medium was changed every 2 d for all differentiation experiments. To calculate the number of osteoclasts, the cells were fixed in acetone and stained for TRAP using an acid phosphatase kit (Sigma-Aldrich). TRAP-positive multinucleated cells containing three or more nuclei were considered as osteoclasts.

**Flow cytometry.** M-CSF–derived osteoclast precursor cells were cultured for 24 h with the indicated concentrations of mouse IL-20, mIgG, 7E, or both mouse IL-20 and 7E. The cells were scraped, incubated for 30 min with 5 μg/ml PE-conjugated antibody against mouse RANK (eBioscience) or isotype control antibody, and then analyzed using a flow cytometer (FACSCalibur; BD). To assay RANKL production, MC3T3-E1 cells were stimulated with 200 ng/ml mouse IL-20, trypsinized, and then stained with PE-conjugated antibody against RANKL (eBioscience) for flow cytometric analysis.

**ELISA.** To test the specificity of 7E, cytokines of the IL-10 family (IL-10, -19, -20, -22, -24, and -26) were coated on the plate with various concentrations and analyzed for their binding with 1 μg/ml anti–IL-20 monoclonal antibody 7E using direct ELISA. To measure serum marker of bone turnover, blood from mice was collected and centrifuged (2,000 rpm for 10 min at 4°C), and serum was collected and stored at −80°C immediately. Serum CTX was determined using a CTX ELISA kit (Nordic Bioscience Diagnostics). Serum osteocalcin, a biochemical parameter of bone formation, was measured using an osteocalcin ELISA kit (Nordic Bioscience Diagnostics). To analyze the enzyme activity of IL-20–treated OC CM, M-CSF–derived osteoclast precursors were cultured with 40 ng/ml of mouse M-CSF and 100 ng/ml sRANKL (PeproTech) for 8 d to become mature multinucleated osteoclast. Mature osteoclasts were washed twice with fresh serum-free α-MEM to make sure there was no residual sRANKL on the osteoclast. Mature osteoclast were treated with PBS or 100–200 ng/ml mouse IL-20 in α-MEM containing 5% FBS for 20 h, and then the OC CM was collected for incubation with osteoblasts. Osteoblastic MC3T3-E1 cells were incubated with control OC CM, mIL-20–treated OC CM, or directly exposed to 100–200 ng/ml mouse IL-20 for 20 h. The culture medium was then collected and sRANKL was determined using RANKL ELISA kit (PeproTech). Cathepsin G-specific inhibitor, *N*-tosyl-L-phenylalanine chloromethyl ketone (TPCK; Sigma-Aldrich) was used to block the protease activity of cathepsin G. 10 μM TPCK dissolved in ethanol was preincubated with control OC CM or mIL-20–treated OC CM for 1 h at 37°C before MC3T3-E1 culture for 20 h. sRANKL concentration in the final culture medium was determined by ELISA.

**Western blot.** MC3T3-E1 cells were stimulated with 200 ng/ml of mouse IL-20 (R&D Systems) for the indicated times. Western blotting, done using the manufacturer's instructions, used antibodies specific for phosphorylated ERK, AKT, STAT3, p38, and JNK (Cell Signaling Technology). Total ERK, AKT, STAT3, p38, and JNK, used as internal controls, were detected using specific antibodies. For osteoclastogenic signal analysis, M-CSF–derived osteoclast precursor cells from IL-20R1$^{+/+}$ and IL-20R1$^{-/-}$ mice were cultured with 200 ng/ml mouse IL-20 for different times, and cell lysates were collected and analyzed using immunoblotting with specific antibodies: TRAF6 (Epitomics), c-Fos (Santa Cruz Biotechnology, Inc.), NFATc1 (Santa Cruz Biotechnology, Inc.), phospho–NF-κB (Cell Signaling Technology), and phospho-STAT3 (Cell Signaling Technology). To assay the inhibitory effect of 7E on osteoclastogenic signals, bone marrow–derived HSCs from WT mice were incubated for 48 h with 40 ng/ml M-CSF and either 2 μg/ml 7E or 2 μg/ml of control mIgG. The cells were then treated with 50 ng/ml sRANKL for 48 h. Cell lysates were collected for osteoclastogenic signal analysis.

**Generating IL-20R1 knockout mice.** A 14-kb IL-20R1 locus subclone was sequenced and found to contain exon 2. A targeting vector containing a 6.3-kb NotI and EcoRI fragment (5′ region of homology) and a 4.2-kb BamHI and SpeI fragment (3′ region of homology) was constructed. Exon 2 was replaced in the targeted locus with a loxP-flanked Neo cassette driven by an HSV-TK promoter in the opposite direction of IL-20R1. The targeting vector was electroporated into C57BL/6 embryonic stem cells and, using nested-set PCR analysis, G418-resistant colonies were screened for homologous recombination. Positive colonies were expanded, and that the 5′ and 3′ arms were targeting the locus was confirmed using Southern blotting with probes flanking the targeting arms. Transient transfection with a plasmid expressing Cre recombinase deleted the Neo cassette. A PCR genotyping strategy to distinguish IL-20R1$^{+/+}$ versus IL-20R1$^{+/-}$ versus IL-20R1$^{-/-}$ was established using specific primers. IL-20R1$^{-/-}$, IL-20R1$^{+/-}$, and WT controls were maintained on a B6 background. IL-20R1$^{+/+}$, IL-20R1$^{+/-}$, and IL-20R1$^{-/-}$ mice were OVX or sham operated. Their tibias were analyzed using micro-CT or else paraffin-sectioned for TRAP staining. The slides were counterstained with hematoxylin.

**Primary osteoblast culture.** Primary osteoblasts were isolated from calvaria of 1-d-old mice by serial digestion (Datta et al., 2005). In brief, calvaria was dissected and subjected to sequential digestions in 2 mg/ml collagenase A and 0.25% trypsin for 20, 40, and 90 min. Cells from the third digestion were rinsed, counted, and plated in α-MEM at a density of 20,000/cm$^2$. Primary cultures were used without passage.

**Isolation of CD11b$^+$ monocytes.** Single-cell suspensions of the spleen were obtained by mechanically disrupting the tissue with a syringe plunger in serum-free α-MEM. Red blood cells were removed using ACK lysing buffer. Splenocytes were labeled with IMag (BD) anti–mouse CD11b beads according to the manufacturer's instructions. After labeling, the cells were separated using the IMagnet (BD), and the positive (CD11b$^+$) fractions were collected and resuspended in α-MEM containing 10% FBS. The purity of CD11b$^+$ monocyte was verified to be greater than 94% by FACS analysis.

**Osteoblast differentiation and co-culture of osteoblasts with osteoclast precursors.** Osteoblast differentiation from primary calvarial cells was induced by culturing in α-MEM containing 10% FBS, 200 μM ascorbic acid, 10 mM β-glycerophosphate, and 10 nM dexamethasone (Sigma-Aldrich). The culture media was replaced once every 2 d. Osteoblast differentiation was evaluated and confirmed by the measurement of alkaline phosphatase and alizarin red S staining. Co-culture of osteoblasts with osteoclast precursors was performed by adding CD11b$^+$ monocytes ($5 \times 10^4$ cells/well) onto the layer of mature osteoblasts (20,000/cm$^2$) and incubated for 9 d in α-MEM supplemented with 10% FBS and 10 nM vitamin D3 (Sigma-Aldrich). To calculate the number of osteoclasts, the cells were fixed in acetone and stained for TRAP using an acid phosphatase kit (Sigma-Aldrich). TRAP-positive multinucleated cells containing three or more nuclei were considered as osteoclasts.

**Statistical analysis.** Prism 5.0 (GraphPad Software) was used for the statistical analysis. A one-way ANOVA nonparametric test (Kruskal-Wallis test) was used to compare the data between groups. Post hoc comparisons were done using Dunn's multiple comparison test. The results of serum IL-20 level in osteoporosis patients are expressed as box plots. Each box represents the 25–75th percentiles. Lines outside the boxes represent the 10th and the 90th percentiles. Lines inside the boxes represent the median. Other results are expressed means ± SD. P-values $<0.05$ were considered significant.

**Online supplemental material.** Fig. S1 shows anti–IL-20 monoclonal antibody 7E protected mice from OVX-induced bone loss. Fig. S2 describes the generation of IL-20R1 knockout mice. Fig. S3 shows the histomorphometric parameters and RANKL/RANK expression in the tibias of IL-20R1$^{-/-}$ mice. Fig. S4 demonstrates IL-20R1 deficiency inhibited osteoclast differentiation and inhibited IL-20–induced osteoclast differentiation in vitro. Fig. S5 shows IL-20R1 deficiency affected both osteoclast precursors and osteoblasts that impaired osteoclast differentiation. Fig. S6 demonstrates IL-20R1 deficiency protected mice from OVX-induced bone loss. Table S1 shows clinical information in patients with osteopenia and osteoporosis. Online supplemental material is available at http://www.jem.org/cgi/content/full/jem.20102234/DC1.

All authors declare no conflicts of interest.

**Submitted: 22 October 2010**
**Accepted: 22 July 2011**

## REFERENCES

Blumberg, H., D. Conklin, W.F. Xu, A. Grossmann, T. Brender, S. Carollo, M. Eagan, D. Foster, B.A. Haldeman, A. Hammond, et al. 2001. Interleukin 20: discovery, receptor identification, and role in epidermal function. *Cell*. 104:9–19. doi:10.1016/S0092-8674(01)00187-8

Boyle, W.J., W.S. Simonet, and D.L. Lacey. 2003. Osteoclast differentiation and activation. *Nature*. 423:337–342. doi:10.1038/nature01658

Caligiuri, G., S.V. Kaveri, and A. Nicoletti. 2006. IL-20 and atherosclerosis: another brick in the wall. *Arterioscler. Thromb. Vasc. Biol.* 26:1929–1930. doi:10.1161/01.ATV.0000237564.81178.bb

Chen, W.Y., and M.S. Chang. 2009. IL-20 is regulated by hypoxia-inducible factor and up-regulated after experimental ischemic stroke. *J. Immunol.* 182:5003–5012. doi:10.4049/jimmunol.0803653

Chen, W.Y., B.C. Cheng, M.J. Jiang, M.Y. Hsieh, and M.S. Chang. 2006. IL-20 is expressed in atherosclerosis plaques and promotes atherosclerosis in apolipoprotein E-deficient mice. *Arterioscler. Thromb. Vasc. Biol.* 26: 2090–2095. doi:10.1161/01.ATV.0000232502.88144.6f

Datta, N.S., C. Chen, J.E. Berry, and L.K. McCauley. 2005. PTHrP signaling targets cyclin D1 and induces osteoblastic cell growth arrest. *J. Bone Miner. Res.* 20:1051–1064. doi:10.1359/JBMR.050106

Dumoutier, L., C. Leemans, D. Lejeune, S.V. Kotenko, and J.C. Renauld. 2001. Cutting edge: STAT activation by IL-19, IL-20 and mda-7 through IL-20 receptor complexes of two types. *J. Immunol.* 167:3545–3549.

Feldmann, M., F.M. Brennan, B.M. Foxwell, and R.N. Maini. 2001. The role of TNF alpha and IL-1 in rheumatoid arthritis. *Curr. Dir. Autoimmun.* 3:188–199. doi:10.1159/000060522

Heuzé-Vourc'h, N., M. Liu, H. Dalwadi, F.E. Baratelli, L. Zhu, L. Goodglick, M. Põld, S. Sharma, R.D. Ramirez, J.W. Shay, et al. 2005. IL-20, an anti-angiogenic cytokine that inhibits COX-2 expression. *Biochem. Biophys. Res. Commun.* 333:470–475. doi:10.1016/j.bbrc.2005.05.122

Hsieh, M.Y., W.Y. Chen, M.J. Jiang, B.C. Cheng, T.Y. Huang, and M.S. Chang. 2006. Interleukin-20 promotes angiogenesis in a direct and indirect manner. *Genes Immun.* 7:234–242. doi:10.1038/sj.gene.6364291

Hsing, C.H., C.L. Ho, L.Y. Chang, Y.L. Lee, S.S. Chuang, and M.S. Chang. 2006. Tissue microarray analysis of interleukin-20 expression. *Cytokine*. 35:44–52. doi:10.1016/j.cyto.2006.07.006

Hsu, Y.H., H.H. Li, M.Y. Hsieh, M.F. Liu, K.Y. Huang, L.S. Chin, P.C. Chen, H.H. Cheng, and M.S. Chang. 2006. Function of interleukin-20 as a proinflammatory molecule in rheumatoid and experimental arthritis. *Arthritis Rheum.* 54:2722–2733. doi:10.1002/art.22039

Jordan, W.J., J. Eskdale, M. Boniotto, G.P. Lennon, J. Peat, J.D. Campbell, and G. Gallagher. 2005. Human IL-19 regulates immunity through auto-induction of IL-19 and production of IL-10. *Eur. J. Immunol.* 35:1576–1582. doi:10.1002/eji.200425317

Ju, J.H., M.L. Cho, Y.M. Moon, H.J. Oh, J.S. Park, J.Y. Jhun, S.Y. Min, Y.G. Cho, K.S. Park, C.H. Yoon, et al. 2008. IL-23 induces receptor activator of NF-kappaB ligand expression on CD4+ T cells and promotes osteoclastogenesis in an autoimmune arthritis model. *J. Immunol.* 181:1507–1518.

Kong, Y.Y., H. Yoshida, I. Sarosi, H.L. Tan, E. Timms, C. Capparelli, S. Morony, A.J. Oliveira-dos-Santos, G. Van, A. Itie, et al. 1999. OPGL is a key regulator of osteoclastogenesis, lymphocyte development and lymph-node organogenesis. *Nature*. 397:315–323. doi:10.1038/16852

Kostenuik, P.J. 2005. Osteoprotegerin and RANKL regulate bone resorption, density, geometry and strength. *Curr. Opin. Pharmacol.* 5:618–625. doi:10.1016/j.coph.2005.06.005

Li, H.H., Y.H. Hsu, C.C. Wei, P.T. Lee, W.C. Chen, and M.S. Chang. 2008. Interleukin-20 induced cell death in renal epithelial cells and was associated with acute renal failure. *Genes Immun.* 9:395–404. doi:10.1038/gene.2008.28

Li, J., I. Sarosi, X.Q. Yan, S. Morony, C. Capparelli, H.L. Tan, S. McCabe, R. Elliott, S. Scully, G. Van, et al. 2000. RANK is the intrinsic hematopoietic cell surface receptor that controls osteoclastogenesis and regulation of bone mass and calcium metabolism. *Proc. Natl. Acad. Sci. USA*. 97:1566–1571. doi:10.1073/pnas.97.4.1566

Liu, L., C. Ding, W. Zeng, J.G. Heuer, J.W. Tetreault, T.W. Noblitt, G. Hangoc, S. Cooper, K.A. Brune, G. Sharma, et al. 2003. Selective enhancement of multipotential hematopoietic progenitors in vitro and in vivo by IL-20. *Blood*. 102:3206–3209. doi:10.1182/blood-2003-05-1419

McClung, M.R. 2006. Inhibition of RANKL as a treatment for osteoporosis: preclinical and early clinical studies. *Curr. Osteoporos. Rep.* 4:28–33. doi:10.1007/s11914-006-0012-7

McClung, M. 2007. Role of RANKL inhibition in osteoporosis. *Arthritis Res. Ther.* 9:S3. doi:10.1186/ar2167

Menaa, C., N. Kurihara, and G.D. Roodman. 2000. CFU-GM-derived cells form osteoclasts at a very high efficiency. *Biochem. Biophys. Res. Commun.* 267:943–946. doi:10.1006/bbrc.1999.2042

O'Brien, C.A. 2010. Control of RANKL gene expression. *Bone*. 46:911–919. doi:10.1016/j.bone.2009.08.050

O'Gradaigh, D., D. Ireland, S. Bord, and J.E. Compston. 2004. Joint erosion in rheumatoid arthritis: interactions between tumour necrosis factor alpha, interleukin 1, and receptor activator of nuclear factor kappaB ligand (RANKL) regulate osteoclasts. *Ann. Rheum. Dis.* 63:354–359. doi:10.1136/ard.2003.008458

Otkjaer, K., K. Kragballe, C. Johansen, A.T. Funding, H. Just, U.B. Jensen, L.G. Sørensen, P.L. Nørby, J.T. Clausen, and L. Iversen. 2007. IL-20 gene expression is induced by IL-1beta through mitogen-activated protein kinase and NF-kappaB-dependent mechanisms. *J. Invest. Dermatol.* 127: 1326–1336. doi:10.1038/sj.jid.5700713

Park, B.K., H. Zhang, Q. Zeng, J. Dai, E.T. Keller, T. Giordano, K. Gu, V. Shah, L. Pei, R.J. Zarbo, et al. 2007. NF-kappaB in breast cancer cells promotes osteolytic bone metastasis by inducing osteoclastogenesis via GM-CSF. *Nat. Med.* 13:62–69. doi:10.1038/nm1519

Pestka, S., C.D. Krause, D. Sarkar, M.R. Walter, Y. Shi, and P.B. Fisher. 2004. Interleukin-10 and related cytokines and receptors. *Annu. Rev. Immunol.* 22:929–979. doi:10.1146/annurev.immunol.22.012703.104622

Ross, F.P., and S.L. Teitelbaum. 2005. alphavbeta3 and macrophage colony-stimulating factor: partners in osteoclast biology. *Immunol. Rev.* 208:88–105. doi:10.1111/j.0105-2896.2005.00331.x

Sa, S.M., P.A. Valdez, J. Wu, K. Jung, F. Zhong, L. Hall, I. Kasman, J. Winer, Z. Modrusan, D.M. Danilenko, and W. Ouyang. 2007. The effects of IL-20 subfamily cytokines on reconstituted human epidermis suggest potential roles in cutaneous innate defense and pathogenic adaptive immunity in psoriasis. *J. Immunol.* 178:2229–2240.

Sato, K., A. Suematsu, K. Okamoto, A. Yamaguchi, Y. Morishita, Y. Kadono, S. Tanaka, T. Kodama, S. Akira, Y. Iwakura, et al. 2006. Th17 functions as an osteoclastogenic helper T cell subset that links T cell activation and bone destruction. *J. Exp. Med.* 203:2673–2682. doi:10.1084/jem.20061775

Simonet, W.S., D.L. Lacey, C.R. Dunstan, M. Kelley, M.S. Chang, R. Lüthy, H.Q. Nguyen, S. Wooden, L. Bennett, T. Boone, et al. 1997. Osteoprotegerin: a novel secreted protein involved in the regulation of bone density. *Cell*. 89:309–319. doi:10.1016/S0092-8674(00)80209-3

Suda, T., N. Takahashi, N. Udagawa, E. Jimi, M.T. Gillespie, and T.J. Martin. 1999. Modulation of osteoclast differentiation and function by the new members of the tumor necrosis factor receptor and ligand families. *Endocr. Rev.* 20:345–357. doi:10.1210/er.20.3.345

Takayanagi, H., K. Sato, A. Takaoka, and T. Taniguchi. 2005. Interplay between interferon and other cytokine systems in bone metabolism. *Immunol. Rev.* 208:181–193. doi:10.1111/j.0105-2896.2005.00337.x

Theill, L.E., W.J. Boyle, and J.M. Penninger. 2002. RANK-L and RANK: T cells, bone loss, and mammalian evolution. *Annu. Rev. Immunol.* 20:795–823. doi:10.1146/annurev.immunol.20.100301.064753

Tritsaris, K., M. Myren, S.B. Ditlev, M.V. Hübschmann, I. van der Blom, A.J. Hansen, U.B. Olsen, R. Cao, J. Zhang, T. Jia, et al. 2007. IL-20 is an arteriogenic cytokine that remodels collateral networks and improves functions of ischemic hind limbs. *Proc. Natl. Acad. Sci. USA*. 104:15364–15369. doi:10.1073/pnas.0707302104

Wada, T., T. Nakashima, N. Hiroshi, and J.M. Penninger. 2006. RANKL-RANK signaling in osteoclastogenesis and bone disease. *Trends Mol. Med.* 12:17–25. doi:10.1016/j.molmed.2005.11.007

Walsh, N.C., T.N. Crotti, S.R. Goldring, and E.M. Gravallese. 2005. Rheumatic diseases: the effects of inflammation on bone. *Immunol. Rev.* 208:228–251. doi:10.1111/j.0105-2896.2005.00338.x

Wei, C.C., W.Y. Chen, Y.C. Wang, P.J. Chen, J.Y. Lee, T.W. Wong, W.C. Chen, J.C. Wu, G.Y. Chen, M.S. Chang, and Y.C. Lin. 2005. Detection of IL-20 and its receptors on psoriatic skin. *Clin. Immunol.* 117:65–72. doi:10.1016/j.clim.2005.06.012

Wei, C.C., Y.H. Hsu, H.H. Li, Y.C. Wang, M.Y. Hsieh, W.Y. Chen, C.H. Hsing, and M.S. Chang. 2006. IL-20: biological functions and clinical implications. *J. Biomed. Sci.* 13:601–612. doi:10.1007/s11373-006-9087-5

Wilson, T.J., K.C. Nannuru, M. Futakuchi, A. Sadanandam, and R.K. Singh. 2008. Cathepsin G enhances mammary tumor-induced osteolysis by generating soluble receptor activator of nuclear factor-kappaB ligand. *Cancer Res.* 68:5803–5811. doi:10.1158/0008-5472.CAN-07-5889

Wilson, T.J., K.C. Nannuru, and R.K. Singh. 2009. Cathepsin G recruits osteoclast precursors via proteolytic activation of protease-activated receptor-1. *Cancer Res.* 69:3188–3195. doi:10.1158/0008-5472.CAN-08-1956